Chemical Science

ROYAL SOCIETY OF CHEMISTRY

EDGE ARTICLE

View Article Online
View Journal | View Issue

Cite this: *Chem. Sci.*, 2024, **15**, 6397

All publication charges for this article have been paid for by the Royal Society of Chemistry

Received 2nd March 2024
Accepted 26th March 2024

DOI: 10.1039/d4sc01469c

rsc.li/chemical-science

Hypocretenolides: collective total syntheses and activities toward metastatic colon cancer†

Bolin Chen,[a] Xijing Zhang,[a] Yufen Yang,[b] Dongdong Xu,[b] Qianwei Wu,[b] Shibo Wang,[a] Shiqi Bao,[c] Xuemei Zhang,[c] Yahui Ding,*[a] Liang Wang *[a] and Yue Chen *[a]

A concise and collective synthetic route to hypocretenolides was developed for the first time. This route features one-pot addition-alkylation and intramolecular 1,3-dipolar cycloaddition to efficiently assemble the 5/7/6 ring system. Our syntheses enabled multigram preparation of hypocretenolide which facilitated further biological evaluation. Preliminary CCK-8 cytotoxic results of hypocretenolide indicated its IC_{50} values within 1 μM against 4 colon cancer cell lines. Wound healing and transwell assays suggested the promising inhibitory activities of hypocretenolide toward the migratory capabilities of colon cancer cells *in vitro*. The animal results confirmed that hypocretenolide can inhibit metastasis of colon cancer cells.

Introduction

Colorectal cancer (CRC) represents approximately one-tenth of all diagnosed cancers annually and is the second most prevalent cause of cancer death.[1–3] It is noteworthy that about 20% CRC patients show metastases at the time of their diagnosis and up to half of the patients with initially localized tumors will develop metastases frequently to the regional lymph nodes, liver and lungs.[4] In recent years, the prognosis of metastatic CRC (mCRC) patients has improved significantly with the development of effective therapeutic methods including surgery and novel anticancer drugs.[4,5] However, in most cases, treatment of mCRC remains challenging[5] and novel candidates are demanded clinically.

Our group has long-term interests in identifying drug candidates from herbal terpene leads. We previously developed drug candidate ACT001 (ref. 6) from the sesquiterpene parthenolide, an active component of the traditional western herb *Tanacetum parthenium* (feverfew). The clinical progress of ACT001 (ref. 7) prompted us to investigate other herbal natural products, especially sesquiterpenoid with an α-methylene motif.[8]

Hypocretenolide was first identified in 1982 by Bohlmann *et al.* from *Hypochoeris cretensiss*.[9] Later, several naturally occurring hypocretenolides varying in oxidation states or glycosylation were isolated (Fig. 1).[10] Unlike other guaianolides having 5/7/5 rings embedded with C6 (or C8)–C12 lactones,[11] hypocretenolides share a unique bridged 5/7/6 ring system (C5–C12 lactone) featuring an α-methylene-δ-lactone motif. Moreover, these natural products were reported to have low IC_{50} values against several cancer cell lines and inhibited activation of NF-κB,[12] which was proved to be closely associated with cancer metastasis.[13]

With remarkable potency, it is conceivable that hypocretenolide would serve as a lead compound for the identification of anticancer agents with potential anti-metastasis activities. However, the further evaluation of hypocretenolide has been impeded by the lack of materials. To the best of our knowledge, the total synthesis of any hypocretenolide has not yet been reported, which definitely obstructs its deep-seated SAR studies and the development of promising hypocretenolide-based candidates. Therefore, we started their total syntheses. Here, we report a general and concise synthetic approach that eventually allowed us to achieve the collective total syntheses of four hypocretenolides.

Results and discussion

From a retrosynthetic perspective (Fig. 2), the C14 or C15 oxidation state of compound **11** and C12 and C2 oxidation

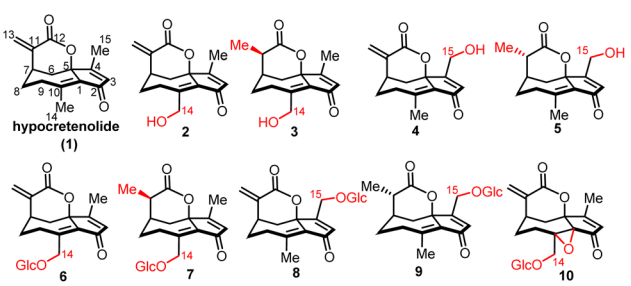

Fig. 1 Representative naturally occurring hypocretenolides.

[a]*State Key Laboratory of Medicinal Chemical Biology, Frontiers Science Center for New Organic Matter, Nankai University, 94 Weijin Road, Tianjin 300071, China. E-mail: 017095@nankai.edu.cn; lwang@nankai.edu.cn; yuechen@nankai.edu.cn*

[b]*College of Pharmacy, Nankai University, 38 Tongyan Road, Tianjin 300353, China*

[c]*Accendatech Co. Ltd, 32nd Floor, Rongqiao Center, Intersection of Changjiang Road and Nankai Six Road, Tianjin 300102, China*

† Electronic supplementary information (ESI) available. CCDC 2280700 and 2280702. For ESI and crystallographic data in CIF or other electronic format see DOI: https://doi.org/10.1039/d4sc01469c

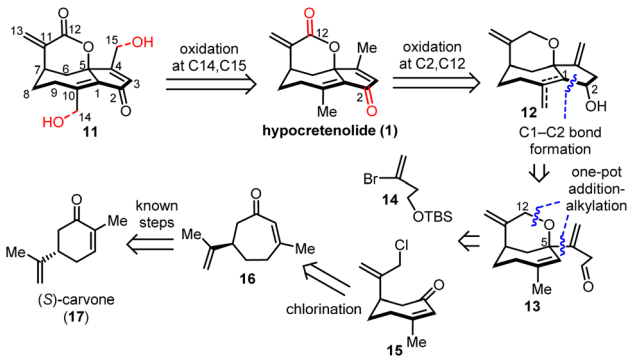

Fig. 2 Retrosynthetic analysis of hypocretenolides.

states of hypocretenolide (**1**) were envisioned to be accessed in the late stage. The 5/7-fused intermediate **12** was anticipated to be built through C1–C2 carbon bond formation from aldehyde **13** using the SmI_2-mediated radical process, Prins reaction or 1,3-dipolar cycloaddition. Aldehyde **13** was further deconstructed into alkene bromide **14** and ketone **15**, which could be combined through an addition of **14**-derived alkene lithium on the ketone group of **15** followed by a tandem alkylation. The ketone **15** could be obtained from the known 7-membered enone **16** *via* an allylic chlorination.

As depicted in Fig. 3, synthesis of compound **16** began with the inexpensive feedstock (*S*)-carvone and involved 5 steps including the Corey–Chaykovsky reaction to introduce cyclopropane, $LiAlH_4$ reduction of ketone, ring expansion to form a 7-membered ring, oxidation with Dess–Martin periodinane, and double bond isomerization to form an α, β-unsatured ketone moiety.[14] Notably, we achieved the preparation of **16** on a multidecagram scale in a yield of >50% with 5 steps. With a sufficient amount of **16** in hand, we investigated its chlorination. Among the three conditions (*t*-BuOCl in hexane; NaClO, $CeCl_3 \cdot 7H_2O$ in DCM/H_2O and NaClO, KH_2PO_4 in DCM/H_2O) we tested, the latter one successfully delivered the regioselective allylic chlorinated product **15** in 73% yield. Next, the alkene lithium generated from **14** (ref. 15) nucleophilically attacked the C5 of compound **15**. However, the adduct was found to be unstable during the quenching process according to the TLC analysis. After several attempts, we succeeded in avoiding decomposition utilizing *t*-BuOH to quench the reaction at low temperature. The addition of TBAI to the resulting reaction mixture induced an alkylation to produce a 6/7-fused intermediate which without chromatography purification was subjected to desilylation. The three successive transformations were achieved in 30% yield to afford alcohol **18** on a multigram scale. Oxidation of **18** with DMP provided aldehyde **13** in 80% yield.

We next aimed at the C1–C2 bond formation to construct the desired 5/6/7 ring system. Attempts with Lewis acids ($BF_3 \cdot Et_2O$, $SnCl_4$, Me_2AlCl or $ZnCl_2$) for the Prins reaction[16] were all fruitless, with the substrate decomposed or intact. We turned our attention to the powerful radical process to connect the C1–C2 carbon bond. However, the aldehyde radical mediated by SmI_2 failed to deliver the desired 5/7/6-membered ring. To our delight, aldehyde **13** was treated with $NH_2OH \cdot HCl$ to afford an oxime intermediate, which was subjected to NaClO conditions and an intramolecular 1,3-dipolar cycloaddition[17] proceeded smoothly to give rise to an isoxazoline product, whose configuration was verified by X-ray crystallography analysis.

With the desired skeleton settled, we moved on to the oxidation adjustment. First, we investigated the reduction of the isoxazoline ring. To our pleasure, the optimal conditions (Fe, AcOH, EtOH/H_2O, 80 °C) we identified provided successful reduction of the O–N bond, accompanied by three transformations including hydrolysis of imine, C4–C15 double bond

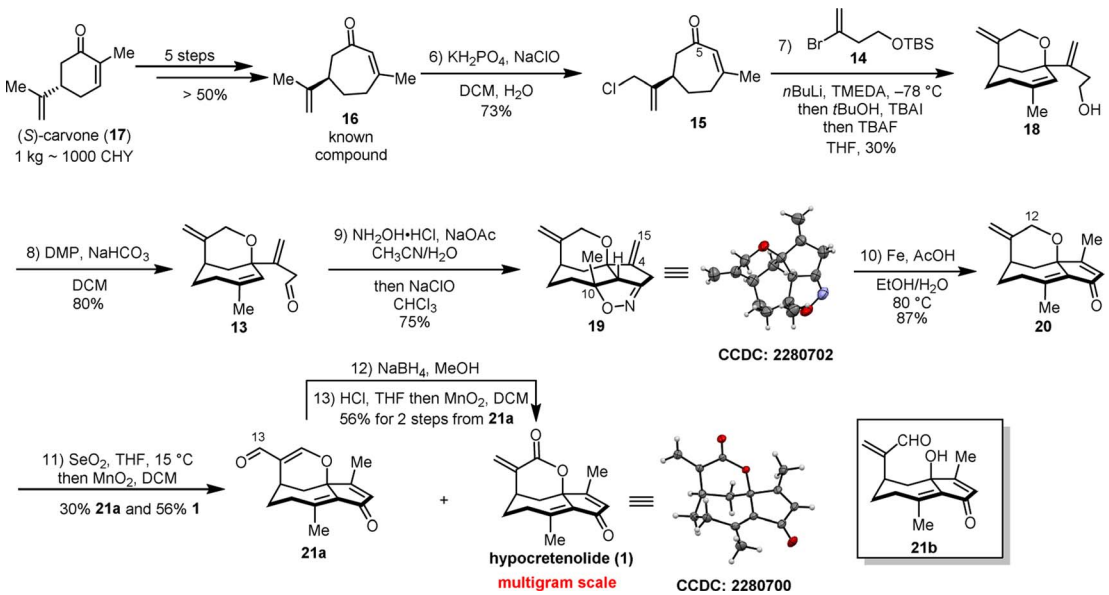

Fig. 3 Total synthesis of hypocretenolide. TMEDA = *N*,*N*,*N*′,*N*′-tetramethylethylenediamine, TBAI = tetrabutylammonium iodide, TBAF = tetrabutyl ammonium fluoride, and DMP = Dess–Martin periodinane.

migration and C10–OH elimination in one pot which eventually delivered the desired dienone **20** in high yield on a gram scale. Then, to introduce the C12 oxidation state, we investigated various conditions (see Table S1 in the ESI†). Conditions of (1) CrO_3, 3,5-DMP or pyridine in DCM and (2) PCC, Ac_2O in DCM both favored the undesired C13–O functionality. The other conditions employing chromium, manganese, and ruthenium reagents resulted in either no reaction or messy results. Pleasingly, 2 equivalents of SeO_2 in THF able to first produce a crude containing **21b** which was successively treated with MnO_2 to provide hypocretenolide (**1**) in 56% yield (multigram scale) accompanied by aldehyde **21a** in 30% yield. To harvest natural product hypocretenolide (**1**), aldehyde **21a** was converted to **1** following a three-step procedure including $NaBH_4$ reduction, HCl-mediated rearrangement and MnO_2 oxidation. The structure of hypocretenolide we synthesized was undoubtedly confirmed by X-ray crystallography analysis.

For structural diversification to facilitate further biological evaluations, we focused on the late-stage oxidation to prepare other analogous natural products. We screened several allylic oxidation conditions and identified that C14 was regioselectively oxidized using SeO_2 in refluxing 1,4-dioxane (Fig. 4A). It should be noted that natural products **3** and **2** were successfully obtained using $NaBH_4$ in a temperature and equivalent-controlled manner.

However, we failed to introduce the C15 oxidation state after extensive investigations. Nonetheless, compound **19** was employed and subjected to epoxidation on the C4–C15 double bond (Fig. 4B). The resulting compound **24** was treated with LDA which induced epoxide ring opening to afford alcohol **25**. After silyl protection, compound **28** was prepared following the procedure described above and then underwent desilylprotection to furnish natural product **4** with the C15–OH functionality.

For preliminary evaluation of anti-colon cancer effects, hypocretenolide was tested against CT-26, MC-38, HCT-116 and HT-29 cancer cell lines (Fig. 5A). The sesquiterpene-derived drug candidate ACT001 and 5-FU were selected as positive controls. The IC_{50} values indicated that the inhibitory activities of hypocretenolide were the same order of magnitude compared to those of 5-FU and up to 100-fold superior than those of ACT001.

To evaluate the effects of hypocretenolide on migratory capabilities of colon cancer cells, wound healing assays were performed. The results (Fig. 5B and C) showed that the scratch wound healing rate significantly dropped after cells were treated with hypocretenolide (1 μM) for both 24 h or 48 h in comparison with those of ACT001 and 5-FU. To further validate the anti-migration effects, transwell assays were conducted and the results (Fig. 5D–F) indicated that the migration and invasion in hypocretenolide-treated groups (0.5 and 1 μM) were obviously decreased when compared with those of ACT001 and 5-FU groups. It is well established that cancer cell migration, which might lead to poor prognosis, could be negatively associated with E-cadherin expression and positively associated with vimentin expression.[18] Based on the results of western blot assays (Fig. 5G and H), E-cadherin expression was clearly increased and vimentin expression was decreased after the cells were treated with hypocretenolide. All the results above suggested the potential inhibitory activities of hypocretenolide toward the migratory capabilities of colon cancer cells *in vitro*.

Furthermore, we employed a liver metastasis mouse model and pulmonary metastasis mouse model to evaluate the effects of hypocretenolide *in vivo*. In the liver metastasis animal model, the CT-26-luci cells initially injected into the spleen of BAL B/c mice could be transferred to the liver. After administration for several days, the bioluminescence intensities in livers which represent the degree of metastasis were detected and the results

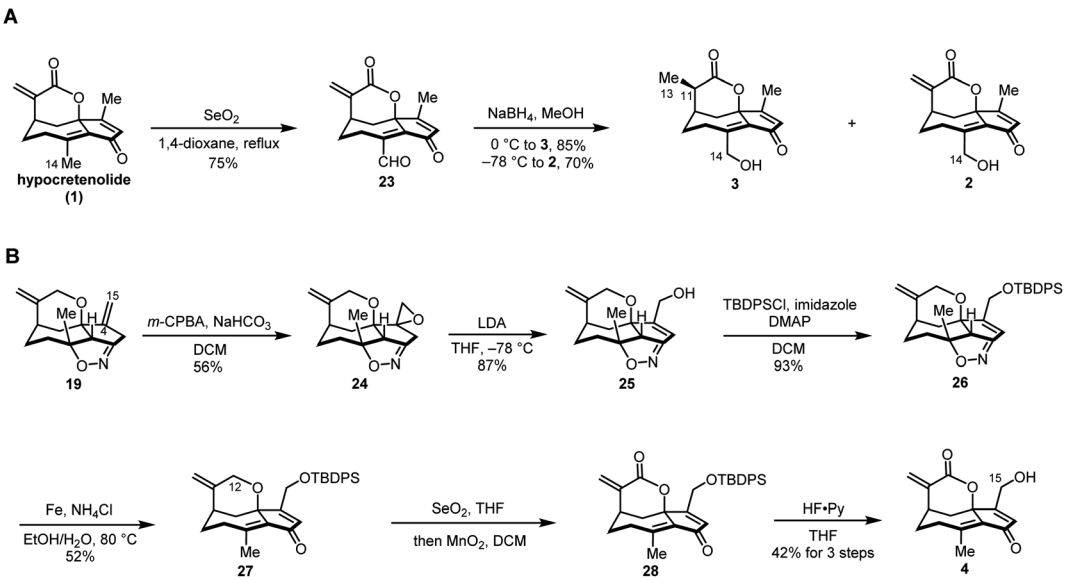

Fig. 4 Syntheses of **2**, **3** and **4**. *m*-CPBA = *meta*-chloroperoxybenzoic acid, LDA = lithium diisopropylamide, and TBDPSCl = *tert*-butylchlorodiphenylsilane.

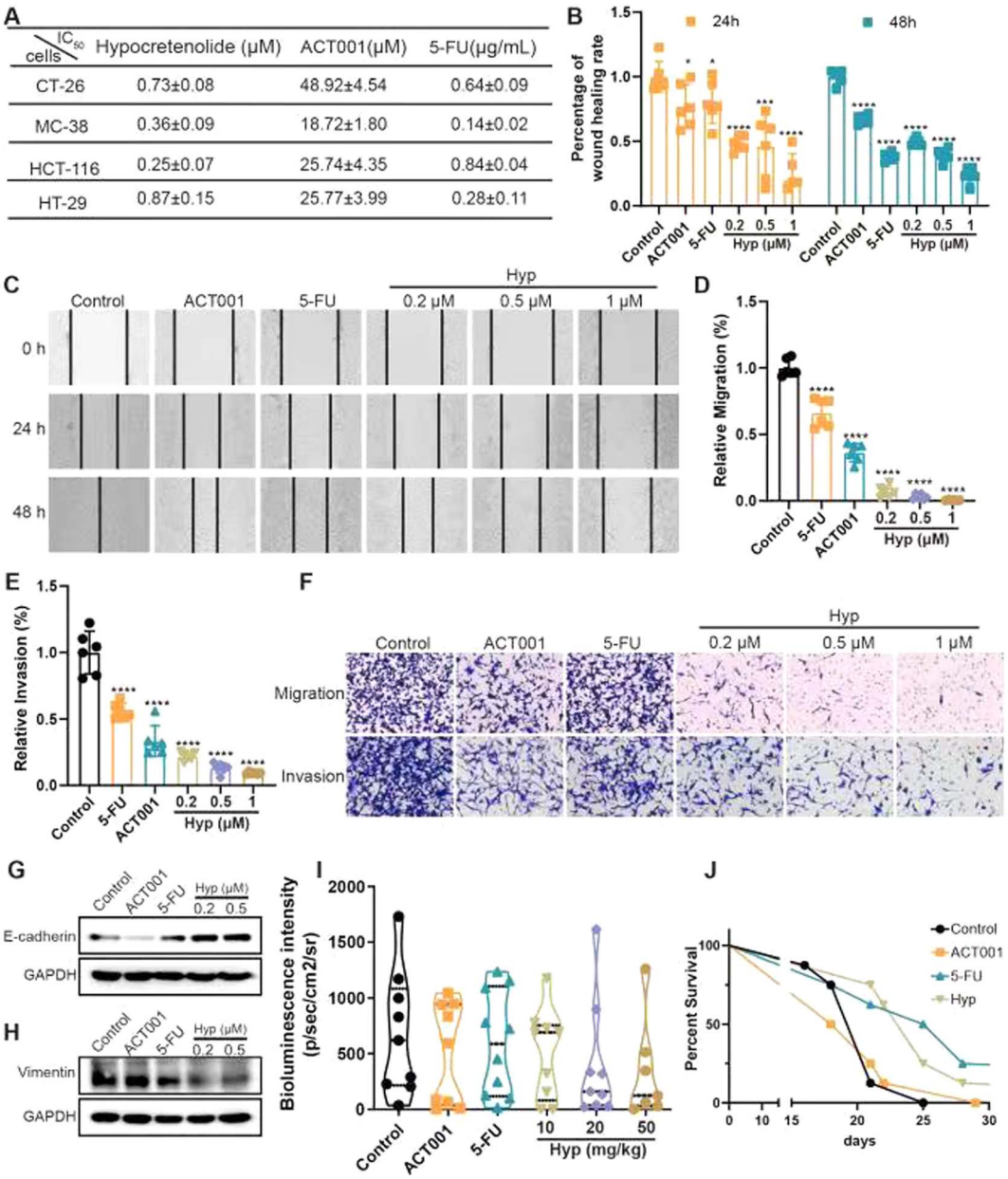

Fig. 5 Hypocretenolide (Hyp) inhibited metastasis of colon cancer cells. (A) The IC_{50} values of hypocretenolide, ACT001 and 5-FU against colon cancer cells; (B and C) the statistical and representative pictures of wound healing assays; (D–F) the statistical and representative pictures of transwell assays; (G and H) western blot assays of E-cadherin and vimentin; (I) the bioluminescence intensities in a liver metastasis mouse model; (J) the survival rate curve in a pulmonary metastasis mouse model.

cells \ IC_{50}	Hypocretenolide (μM)	ACT001(μM)	5-FU(μg/mL)
CT-26	0.73±0.08	48.92±4.54	0.64±0.09
MC-38	0.36±0.09	18.72±1.80	0.14±0.02
HCT-116	0.25±0.07	25.74±4.35	0.84±0.04
HT-29	0.87±0.15	25.77±3.99	0.28±0.11

suggested that the bioluminescence intensities in the hypocretenolide (20 and 50 mg kg^{-1})-treated group were lower compared to that in other groups. As for the pulmonary model, the CT-26-luci cells were injected into BAL B/c mice through the tail vein followed by administration. The survival rates were calculated. The results suggested that hypocretenolide and 5-FU prolonged the survival period of mice compared to ACT001 and the untreated control. These results confirmed that hypocretenolide can ameliorate metastasis of colon cancer cells and potentially exhibit therapeutic benefits, providing us with a new chemical pool for identifying novel anti-colon cancer candidates.

Conclusions

In conclusion, we have achieved a scalable and collective synthetic route to the hypocretenolide scaffold. The key transformations include the one-pot addition-alkylation and 1,3-dipolar cycloaddition to rapidly construct the 5/7/6 ring system. It is conceived that the 11–15 step synthetic route we developed is applicable not only to the preparation of other hypocretenolides, but also to the derivatives (*e.g.* C14 or C15–OH derivatives) not available in nature. More importantly, we discovered the anti-mCRC effects of hypocretenolide *in vitro* and *in vivo* based on the data of wound healing assays, transwell

assays and animal experiments. All the results suggested that the hypocretenolide scaffold opens an avenue for the discovery of novel anti-mCRC candidates.

Data availability

The datasets supporting this article have been uploaded as part of the ESI.†

Author contributions

B. Chen, X. Zhang, Y. Yang, D. Xu, Q. Wu, and S. Wang carried out the chemical synthesis. S. Bao and X. Zhang contributed to the biological experiments. B. Chen, Y. Ding, L. Wang, and Y. Chen supervised the project and wrote and revised the manuscript.

Conflicts of interest

The authors declare no competing financial interest.

Acknowledgements

This research was made possible as a result of a generous grant from the National Natural Science Foundation of China (NSFC, grant no. 82273794 and 82073695), the Frontiers Science Center for New Organic Matter, Hundred Young Academic Leaders Program of Nankai University (grant no. 63233023), and the China Postdoctoral Science Foundation (grant no. 2023M731790).

Notes and references

1 F. Bray, J. Ferlay, I. Soerjomataram, R. L. Siegel, L. A. Torre and A. Jemal, *Ca-Cancer J. Clin.*, 2018, **68**, 394–424.
2 E. Dekker, P. J. Tanis, J. L. A. Vleugels, P. M. Kasi and M. B. Wallace, *Lancet*, 2019, **394**, 1467–1680.
3 L. H. Biller and D. Schrag, *JAMA*, 2021, **25**, 669–685.
4 F. Ciardiello, D. Ciardiello, G. Martini, S. Napolitano, J. Tabernero and A. Cervantes, *Ca-Cancer J. Clin.*, 2022, **72**, 372–401.
5 J. E. Riedesser, M. P. Ebert and J. Betge, *Ther. Adv. Med. Oncol.*, 2022, **14**, 17588359211072703.
6 (*a*) Q. Zhang, Y. Lu, Y. Ding, J. Zhai, Q. Ji, W. Ma, M. Yang, H. Fan, J. Long, Z. Tong, Y. Shi, Y. Jia, B. Han, W. Zhang, C. Qiu, X. Ma, Q. Li, Q. Shi, H. Zhang, D. Li, J. Zhang, J. Lin, L. Li, Y. Gao and Y. Chen, *J. Med. Chem.*, 2012, **55**, 8757–8769; (*b*) Y. An, W. Guo, L. Li, C. Xu, D. Yang, S. Wang, Y. Lu, Q. Zhang, J. Zhai, H. Fan, C. Qiu, J. Qi, Y. Chen and S. Yuan, *PLoS One*, 2015, **10**, e0116202.
7 (*a*) **https://www.chictr.org.cn**, register number: ChiCTR2000035315; (*b*) **https://ClinicalTrials.gov**, NCT number: NCT05053880; (*c*) **https://www.anzctr.org.au**, Trial ID: ACTRN12621001172897.
8 A. Ghantous, H. Gali-Muhtasib, H. Vuorela, N. A. Saliba and N. Darwiche, *Drug Discovery Today*, 2010, **15**, 668–678.
9 F. Bohlmann and P. Singh, *Phytochemistry*, 1982, **21**, 2119–2120.
10 (*a*) F. M. Harraz, F. F. Kassem, M. Grenz, J. Jakupovic and F. Bohlmann, *Phytochemistry*, 1988, **27**, 1866–1867; (*b*) C. Zidorn, E. P. Ellmerer-Müller and H. Stuppner, *Phytochemistry*, 1998, **49**, 797–800; (*c*) C. Zidorn, E. P. Ellmerer, G. Konwalinka, K. H. Ongania, R. Schwaha, R. Greil, K. Joehrer, N. B. Perry and H. Stuppner, *Lett. Org. Chem.*, 2005, **2**, 461–464; (*d*) C. Zidorn, R. Spitaler, S. Grass, J. Mader, T. Müller, E. P. Ellmerer and H. Stuppner, *Biochem. Syst. Ecol.*, 2007, **35**, 301–307.
11 For representative reviews of guaianolide syntheses, see: (*a*) A. Santana, J. M. G. Molinillo and F. A. Macías, *Eur. J. Org Chem.*, 2015, **2015**, 2093–2110; (*b*) R. A. Fernandes, S. Moharana and G. N. Khatun, *Org. Biomol. Chem.*, 2023, **21**, 6652–6670; For representative guaianolide syntheses: ; (*c*) S. Carret and J.-P. Deprés, *Angew. Chem., Int. Ed.*, 2007, **46**, 6870–6873; (*d*) S. Kalidindi, W. B. Jeong, A. Schall, R. Bandichhor, B. Nosse and O. Reiser, *Angew. Chem., Int. Ed.*, 2007, **46**, 6361–6363; (*e*) G. Valot, J. Garcia, V. Duplan, C. Serba, S. Barluenga and N. Winssinger, *Angew. Chem., Int. Ed.*, 2012, **51**, 5391–5394; (*f*) C. Li, L. Dian, W. Zhang and X. Lei, *J. Am. Chem. Soc.*, 2012, **134**, 12414–12417; (*g*) T. C. Johnson, M. R. Chin, T. Han, J. P. Shen, T. Rana and D. Siegel, *J. Am. Chem. Soc.*, 2016, **138**, 6068–6073; (*h*) X. Hu, S. Xu and T. J. Maimone, *Angew. Chem., Int. Ed.*, 2017, **56**, 1624–1628; (*i*) D. Chen and P. A. Evans, *J. Am. Chem. Soc.*, 2017, **139**, 6046–6049; (*j*) X. Hu, A. J Musacchio, X. Shen, Y. Tao and T. J. Maimone, *J. Am. Chem. Soc.*, 2019, **141**, 14904–14915; (*k*) F. Kaden and P. Metz, *Org. Lett.*, 2021, **23**, 1344–1348.
12 (*a*) C. Zidorn, H. Stuppner, M. Tiefenthaler and G. Konwalinka, *J. Nat. Prod.*, 1999, **62**, 984–987; (*b*) C. Zidorn, V. M. Dirsch, P. Rüngeler, S. Sosa, R. D. Loggia, I. Merfort, H. L. Pahl, A. M. Vollmar and H. Stuppner, *Planta Med.*, 1999, **65**, 704–708.
13 (*a*) S. Huang, C. A. Pettaway, H. Uehara, C. D. Bucana and I. J. Fidler, *Oncogene*, 2001, **20**, 4188–4197; (*b*) S. Mirzaei, S. Saghari, F. Bassiri, R. Raesi, A. Zarrabi, K. Hushmandi, G. Sethi and V. Tergaonkar, *J. Cell. Physiol.*, 2022, **237**, 2770–2795.
14 M. L. de Faria, R. de A. Magalhães, F. C. Silva, L. G. de O. Matias, M. A. Ceschi, U. Brocksom and T. J. Brocksom, *Tetrahedron: Asymmetry*, 2000, **11**, 4093–4103.
15 B. V. S. Reddy, S. G. Reddy, M. R. Reddy, M. P. Bhadra and A. V. S. Sarma, *Org. Biomol. Chem.*, 2014, **12**, 7257–7260.
16 X. Han, G. Peh and P. E. Floreancing, *Eur. J. Org Chem.*, 2013, **2013**, 1193–1208.
17 M. Ihara, Y. Tokunaga, N. Taniguchi, K. Fukumoto and C. Kabuto, *J. Org. Chem.*, 1991, **56**, 5281–5285.
18 (*a*) S. Xiao, L. Liu, X. Lu, J. Long, X. Zhou and M. Fang, *J. Cancer Res. Clin.*, 2015, **141**, 1465–1474; (*b*) M. M. Nijkamp, P. N. Span, I. J. Hoogsteen, A. J. van der Kogel, J. H. A. M. Kaanders and J. Bussink, *Radiother. Oncol.*, 2011, **99**, 344–348.